iScience

Article

Tumor necrosis factor-stimulated gene-6 inhibits endoplasmic reticulum stress in the ischemic mouse kidney

Graphical abstract

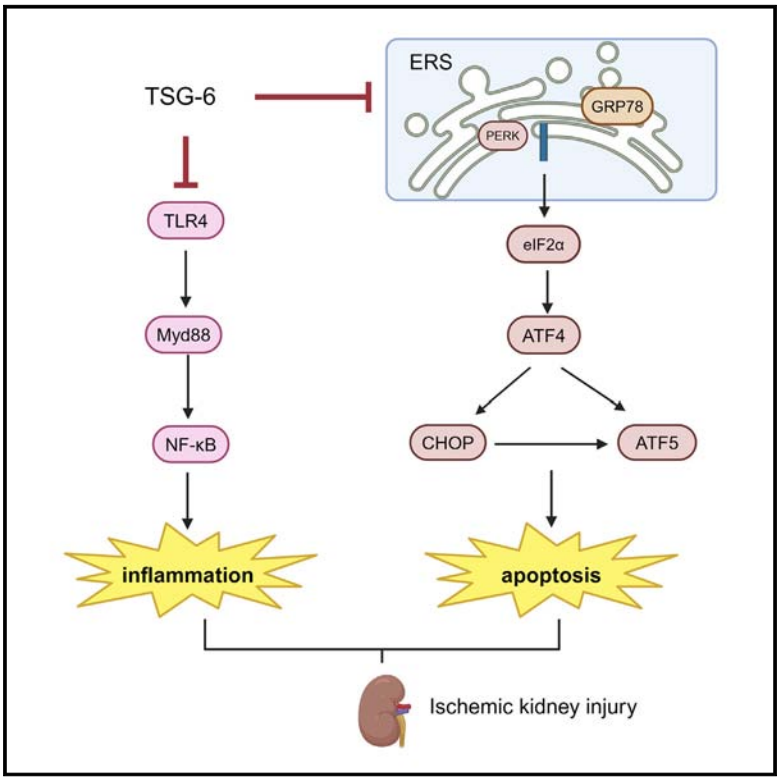

Authors

Bo Lu, Li Xing, Xiang-Yang Zhu, ..., Amir Lerman, Alfonso Eirin, Lilach O. Lerman

Correspondence

lerman.lilach@mayo.edu

In brief

Natural sciences; Biological sciences; Physiology

Highlights

- Ischemic kidney injury involves inflammation and endoplasmic reticulum stress (ERS)
- Tumor necrosis factor-stimulated gene-6 (TSG-6) is an anti-inflammatory molecule
- TSG-6 improved ischemic murine kidney function and decreased inflammation and ERS
- TSG-6 may serve as a therapeutic agent for ischemic kidney disease

Lu et al., 2024, iScience 27, 111454
December 20, 2024
https://doi.org/10.1016/j.isci.2024.111454

CellPress

iScience

CellPress
OPEN ACCESS

Article

Tumor necrosis factor-stimulated gene-6 inhibits endoplasmic reticulum stress in the ischemic mouse kidney

Bo Lu,[1,2] Li Xing,[1,3] Xiang-Yang Zhu,[1] Hui Tang,[1] Brandon Lu,[1] Fei Yuan,[1,4] Yazan Almasry,[1] Alexander Krueger,[1] Samer H. Barsom,[1] James D. Krier,[1] Kyra L. Jordan,[1] Amir Lerman,[5] Alfonso Eirin,[1] and Lilach O. Lerman[1,6,*]

[1]Division of Nephrology and Hypertension, Mayo Clinic, 200 First Street SW, Rochester, MN 55905, USA
[2]Department of Cardiology, Yueyang Hospital of Integrated Traditional Chinese and Western Medicine, Shanghai University of Traditional Chinese Medicine, 110 Ganhe Road, Shanghai 200437, China
[3]Department of Urology, Zhongda Hospital, Southeast University, Nanjing, Jiangsu Province, China
[4]Department of Urology, National Children's Medical Center, Shanghai Children's Medical Center, School of Medicine, Shanghai Jiao Tong University, Shanghai, China
[5]Department of Cardiology, Mayo Clinic, 200 First Street SW, Rochester, MN 55905, USA
[6]Lead contact
*Correspondence: lerman.lilach@mayo.edu
https://doi.org/10.1016/j.isci.2024.111454

SUMMARY

Kidney tissue injury in renal artery stenosis (RAS) involves inflammation, endoplasmic reticulum stress (ERS), and mitochondria damage. Tumor necrosis factor-stimulated gene-6 (TSG-6), an endogenous reparative molecule, may decrease ERS and improve renal function. To assess its impact on the stenotic murine kidney, we injected TSG-6 or vehicle for two weeks in mice with RAS. At completion, we assessed stenotic kidney function and oxygenation, inflammation, and expression of ERS-related genes. TSG-6 treatment reduced renal hypoxia, urinary protein and plasma creatinine levels, renal fibrosis, and apoptosis. TSG-6 also exhibited an anti-inflammatory effect, reflected in the downregulated expression of the Toll-like receptor 4 (TLR4)/nuclear factor κB (NF-κB) pathway in murine kidneys *in vivo* and HK-2 cells *in vitro*. Moreover, ERS-related molecules were downregulated after TSG-6 treatment, while most indicators of mitochondrial unfolded protein response remained unaltered. Therefore, TSG-6 alleviates inflammation, ERS, apoptosis, and fibrosis in the post-stenotic mouse kidney. These observations position TSG-6 as a potential therapeutic tool in RAS.

INTRODUCTION

Renal artery stenosis (RAS) is a leading cause for secondary hypertension and may result in renal tissue damage, dysfunction, and eventually end-stage kidney disease if left untreated.[1] However, while many existing treatments focus on restoring blood flow to the kidney, kidney function does not always recover,[2] likely due to persistent damage to kidney structure.[3] The need to directly repair the post-stenotic kidney arises from tissue damage and irreversible kidney dysfunction, prompting the exploration of alternative techniques.

Inflammation, hypoxia, and fibrosis play pivotal roles in the pathogenesis of ischemic renal damage, and the modulation of inflammatory signaling is a key tenet in therapeutic interventions.[4] We previously found that mesenchymal stem cells (MSCs) improved stenotic kidney injury by alleviating inflammatory responses. Notably, their therapeutic benefits were partly attributed to MSC activation by inflammatory signals from damaged tissues, upregulating the expression of anti-inflammatory protein tumor necrosis factor alpha (TNF-α)-stimulated gene/protein-6 (TSG-6).[5] This small protein (molecular mass ~35–38 kDa) is known for its anti-inflammatory and tissue-protective properties in a variety of disease states, like lung injury,[6] rheumatoid arthritis, or vascular injury.[7] Similarly, TSG-6 restored renal structure and function in experimental rodent models of acute or chronic renal disease.[8–10] Hence, we hypothesized that TSG-6 could potentially ameliorate kidney damage due to RAS.

Furthermore, elevated inflammatory cytokines can trigger the unfolded protein response (UPR), a cellular stress reaction associated with the endoplasmic reticulum (ER).[11] The UPR serves to reduce protein synthesis, accelerate the folding machinery, and increase the degradation of unfolded proteins. Failure of UPR may lead to ER stress (ERS) and in turn increased production of reactive oxygen species, inflammation, and cell death. Many insults, like hypoxia and ischemia, that are encountered upon kidney injury are prone to trigger ERS,[12] which participates in acute and chronic tissue damage.[13] Therefore, regulating ERS in kidney cells may provide a therapeutic target in ischemic kidney damage.[14]

Moreover, inflammation also interplays with mitochondrial stress,[15] and renal ischemia affects the expression of mitochondria-related genes and damages mitochondrial structure and function in swine RAS.[16] The mitochondrial UPR (mtUPR) is a newly discovered process associated with mitochondrial quality control and various cell stresses.[17] Increased expression of

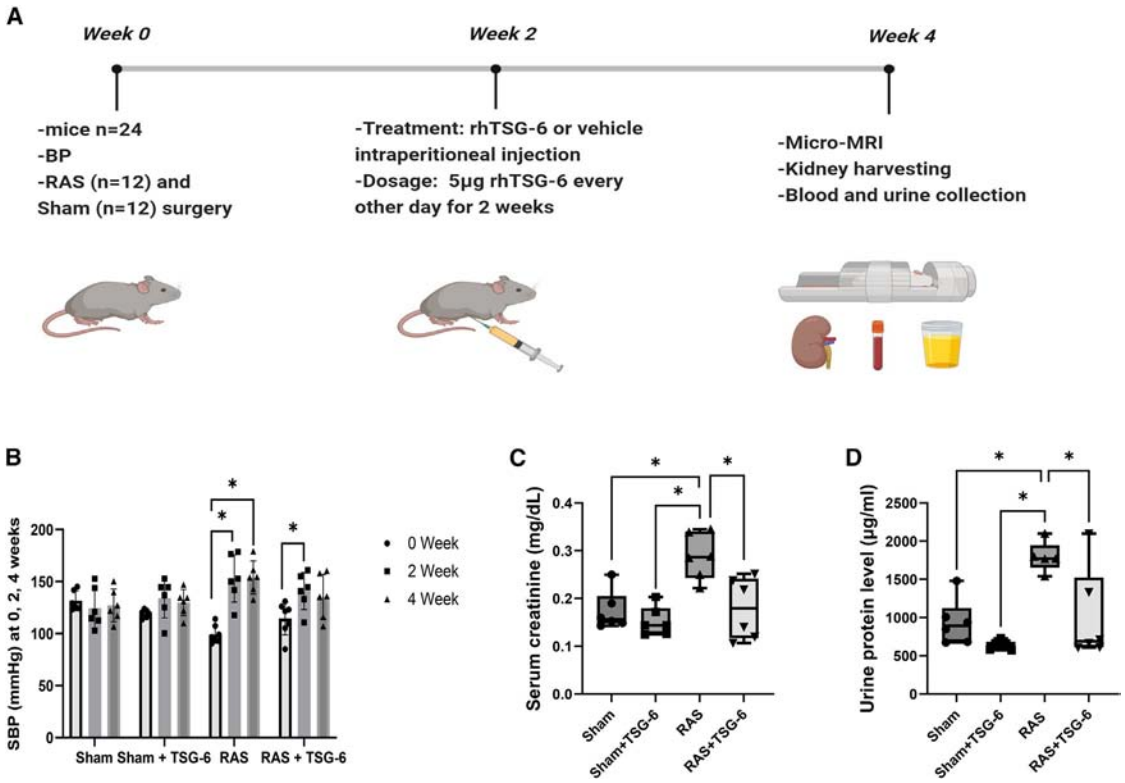

Figure 1. Schematic of the experimental protocol and systemic characteristics of mice after TSG-6 injection

Twenty-four mice were randomly assigned to four groups. Renal artery stenosis (RAS) and sham surgery were performed in 12 mice each. Two weeks later, TSG-6 was administered to RAS and sham mice every other day over two weeks, while control RAS and sham mice received PBS. Blood pressure was measured every 2 weeks. At the completion of treatment, MRI scanning was performed, plasma and urine samples were collected, and kidneys were harvested for *ex vivo* experiments (A). RAS increased in mice systolic blood pressure (SBP) two and four weeks after surgery (B), as well as plasma creatinine (C) and urine protein level (D) at 4 weeks. TSG-6 tended to reduce SBP and blunted the increase of serum creatinine and urine protein levels. Data are represented as mean ± SD. *$p < 0.05$, comparisons were performed using one-way ANOVA followed by Fisher's least significant difference (LSD) test or a paired t test as appropriated, $n = 6$ mice/group.

chaperone proteins and mitochondrial proteases during the mtUPR could change mitochondrial protein dynamics, thus modulating mitochondrial function.[18] Preserving mitochondrial and ER function prevents or delays the fibrotic process and loss of renal function in a unilateral ureteral obstruction model.[19] These observations suggest that targeting the ERS and mitochondrial stress responses could be a potential therapeutic strategy for kidney damage in RAS.

TSG-6 exerts protective effects in spinal cord ischemia-reperfusion damage by inhibiting ERS.[20] However, the potential protective effects of TSG-6 in renal damage induced by RAS, the associated molecular mechanisms, or its ability to modulate ERS in ischemic kidneys remains unclear. Therefore, we tested the hypothesis that TSG-6 administration attenuates inflammatory markers, ERS, and mtUPR in murine RAS, accompanied by reduced renal damage.

RESULTS

Characteristics of mice after TSG-6: Improved stenotic kidney function

RAS surgery resulted in a significant increase in systolic blood pressure (SBP) two weeks post-surgery, indicating successful induction of RAS (Figure 1). By 4 weeks, SBP remained elevated in RAS+vehicle but was no longer different than either baseline or 2 weeks in RAS+TSG-6, (Figure 1). Furthermore, following TSG-6 treatment, serum creatinine ($p < 0.001$) and urinary protein levels ($p = 0.002$) were significantly reduced compared to RAS+vehicle group (Figure 1). Contrarily, stenotic kidney volume did not increase in RAS+TSG-6 vs. RAS, and cortical and medullary perfusion that were lower than sham in RAS remained decreased in RAS+TSG-6 (Figure 2).

On the other hand, MRI revealed that RAS+vehicle had significantly elevated cortical and medullary hypoxia compared to both sham groups, but treatment with TSG-6 in RAS reduced hypoxia to levels similar to sham (Figure 2).

TSG-6 protected the stenotic kidney from fibrosis and apoptosis

Histology showed that TSG-6 treatment ameliorated stenotic kidney tissue damage, as indicated by the decreased fibrosis in RAS+TSG-6 vs. RAS+vehicle ($p < 0.001$) (Figures 3A and 3B), which became comparable to the sham group. The number of apoptotic cells in the stenotic kidneys of RAS mice significantly increased but decreased following TSG-6 treatment ($p = 0.03$ vs. RAS, Figures 3C and 3D).

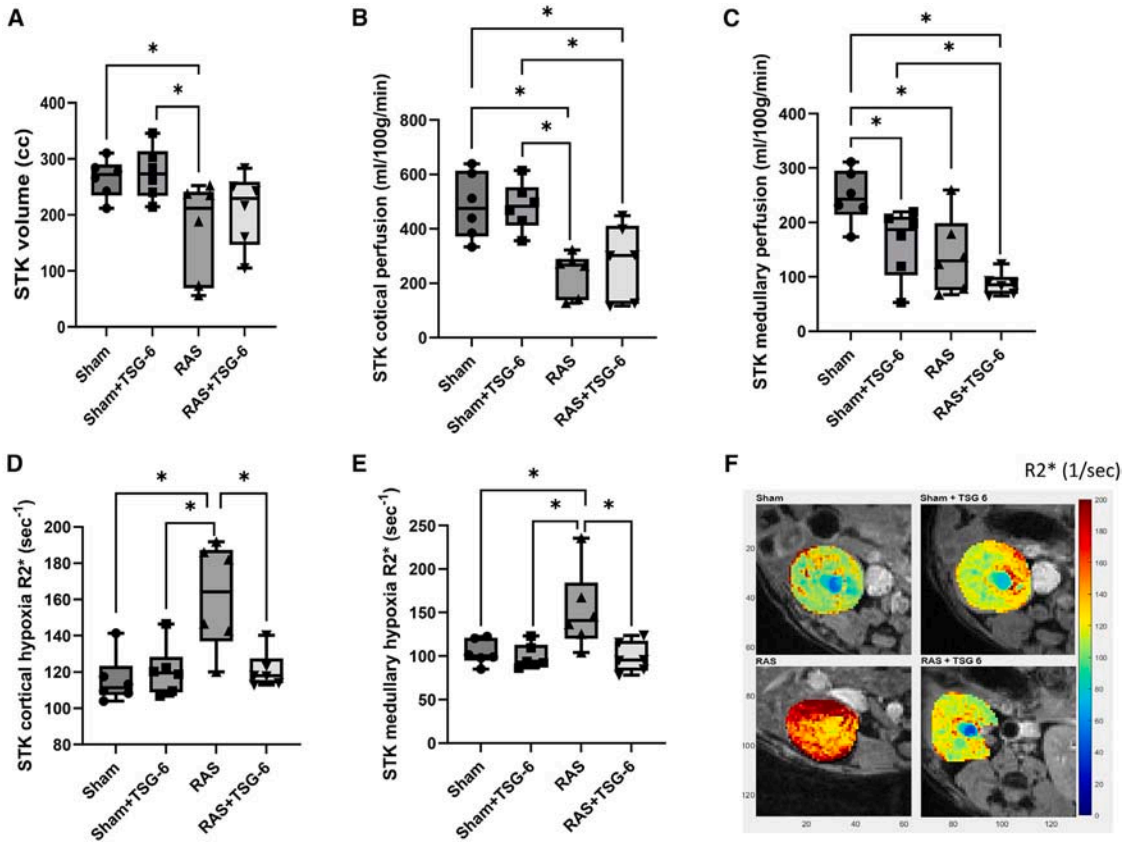

Figure 2. Kidney function obtained using MRI in mice

The stenotic kidney (STK) volume, cortical, and medullary perfusion all decreased in RAS and remained unchanged in RAS+TSG-6 ($p < 0.05$ vs. RAS) (A–C), although renal volume was no longer lower than sham. Cortical and medullary hypoxia measured by BOLD-MRI was evident in RAS. Treatment with TSG-6 significantly decreased kidney hypoxia compared to RAS and became comparable to sham (D and E). Representative BOLD images showing elevated R2* (red regions) in RAS that was remarkably decreased by TSG-6 (F). Data are represented as mean ± SD. *$p < 0.05$, comparisons were performed using one-way ANOVA followed by Fisher's LSD test, $n = 6$ mice/group.

TSG-6 ameliorated renal inflammation

The ratio of M1/M2 in RAS mice significantly increased compared to sham ($p = 0.03$); RAS+TSG-6 showed a trend for decreased M1/M2 ($p = 0.08$), which was no longer different from sham (Figures 3E and 3F). RAS kidneys showed elevated gene and protein expression of the pro-inflammatory cytokine TNF-α, as well as nuclear factor κB (NF-κB) and Toll-like receptor 4 (TLR4). RAS+TSG-6 showed downregulated expression of all the inflammatory markers and TLR4/My88, indicating that the protective effects of TSG-6 may act through the TLR4-mediated inflammatory pathway (Figure 4).

TSG-6 abolished ERS but not mtUPR in stenotic kidneys

We observed upregulated both mRNA and protein expression of C/EBP homologous protein (CHOP) and GRP78 in RAS, indicating ERS was alleviated in RAS+TSG-6 (Figure 4). TSG-6 was mainly expressed in renal tubular and interstitial cells (Figure 4). Importantly, TSG-6 expression was similar in normal and RAS kidneys but boosted in both sham and RAS mice treated with intraperitoneal (i.p.) TSG-6 injections, indicating the treatment efficacy. The transcription factor ATF4 can be associated with either ERS or mtUPR. However, we found no significant changes in the expression of the mtUPR-related genes ClpP, LonP1, Hsp10, or Hsp60 in any group, while the ERS indices protein kinase R-like endoplasmic reticulum kinase (PERK) and eIF2α were also elevated in stenotic RAS kidneys and ameliorated in RAS+TSG-6 (Figure 5), suggesting that TSG-6 eliminated ERS but not mtUPR in stenotic kidneys.

TSG-6 partially inhibits the TLR4/NF-κB inflammatory pathway *in vitro*

In HK-2 cells, lipopolysaccharide (LPS) upregulated both TLR4 and NF-κB expression. TSG-6 treatment alone abolished LPS-stimulated TLR4 and decreased NF-κB expression to levels no longer different from control. The combination of TSG-6 with TLR4 inhibition did not decrease TLR4 any further but additively abolished NF-κB expression. Taken together, these observations suggest that TSG-6 inhibits NF-κB at least partially by inhibiting TLR4 (Figure 5). For comparison, TGS-6 significantly decreased TNF-α expression, whereas TAK-242 alone did not (Figure 5), suggesting that TSG-6's anti-inflammatory effects may not be uniformly achieved only through the TLR4 pathway.

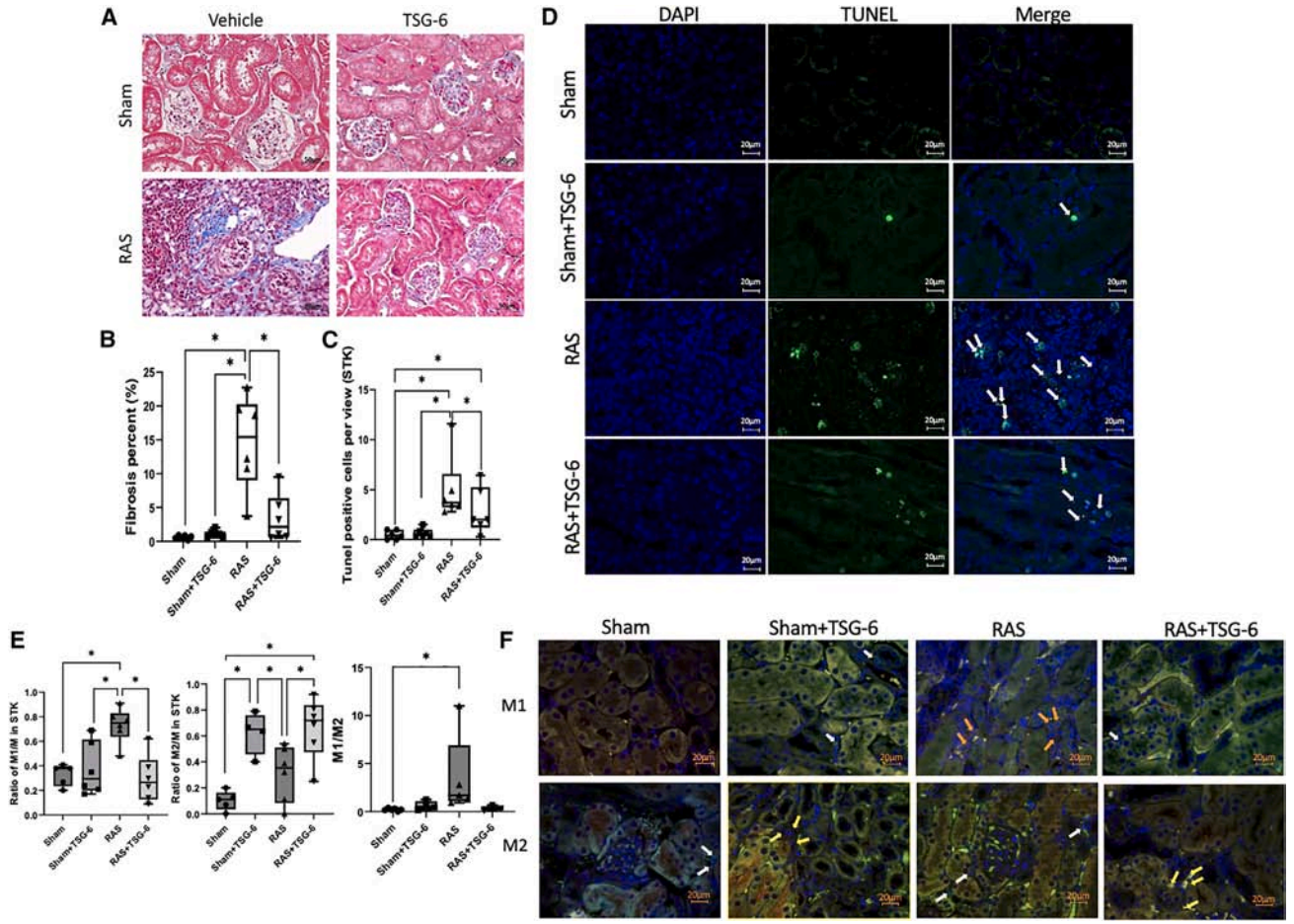

Figure 3. Renal fibrosis and apoptosis in RAS

Quantification of Masson trichrome staining revealed increased renal fibrosis in RAS vs. sham, which was lowered by TSG-6 (both $p < 0.05$) (A and B). TUNEL staining (green, blue nuclei) indicated almost no apoptotic cells in the sham and sham+TSG-6 groups. RAS markedly increased the number of TUNEL+ cells, which TSG-6 significantly decreased (C and D). White arrows show representative TUNEL-positive cells. RAS increased the number of iNOS+/F4/80 + M1 macrophages, which was reduced after TSG-6. A greater number of MRC-1+/F4/80 + M2 macrophages were observed in the stenotic kidney of RAS+TSG-6 vs. RAS. The M1/M2 ratio in RAS was higher than sham, and TSG-6 tended to reduce it (E and F). Orange arrows: M1 macrophages; white arrows: overall macrophages; yellow arrows: M2 macrophages. Data are represented as mean ± SD. *$p < 0.05$, comparisons were performed using one-way ANOVA followed by Fisher's LSD test, $n = 6$ mice/group.

DISCUSSION

This study shows that TSG-6 can ameliorate kidney function in mice with RAS, as demonstrated by the decrease in serum creatinine and urinary protein. TSG-6 also decreased kidney hypoxia and fibrosis and slightly increased kidney volume, although it did not affect cortical or medullary perfusion. Furthermore, TSG-6 downregulated inflammatory marker expression partially through the TLR4/NF-κB pathway and decreased the M1/M2 ratio. In addition, TSG-6 also blunted renal cell apoptosis and ERS (ATF4, ATF5, GRP78, PERK, CHOP, and eIF2α expression). Overall, TSG-6 improved the RAS kidney function and inhibited inflammation and ERS-induced apoptosis. These observations position TSG-6 as a potential therapeutic tool in RAS.

Renovascular hypertension is primarily driven by RAS and can progress to end-stage renal disease. The kidney situated distal to the stenosis exhibits microvascular rarefaction, heightened oxidative stress, inflammation, and interstitial fibrosis.[21] In particular, accumulated macrophages[22,23] and ischemia trigger the release of pro-inflammatory cytokines including interleukin (IL)-1, IL-6, monocyte chemoattractant protein-1 (MCP-1), and TNF-α,[22,24] thereby exacerbating renal damage and fibrosis. We have previously observed that MSCs effectively reduce renal levels of TNF-α and IL-1β, potentially contributing to the improvement in microvascular structure in RAS.[25] This may be partly mediated by secreting TSG-6, which plays a crucial role in anti-inflammation and promoting kidney tissue repair.[5]

TLRs are evolutionarily conserved pattern recognition receptors that play a crucial role in mediating innate and adaptive immune responses. They detect and respond to exogenous injurious ligands and endogenous danger-associated molecular patterns generated following tissue damage.[26] In angiotensin-II-induced hypertensive nephropathy, the interaction between

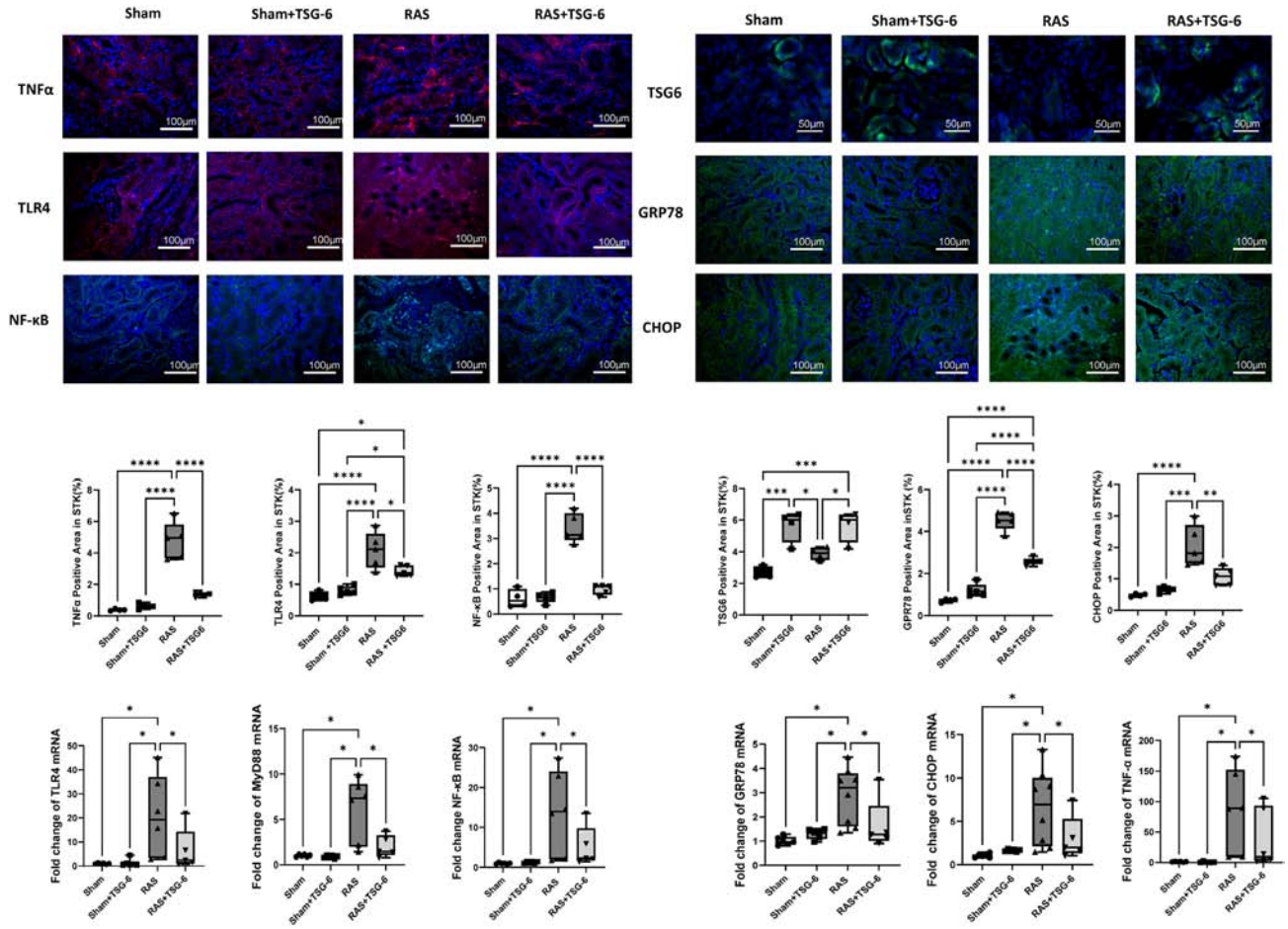

Figure 4. The effect of TSG-6 on kidney inflammation and ERS in RAS

Renal protein expression of TNF-α, TLR4, and NF-κB was upregulated in RAS but markedly decreased in RAS+TSG-6 mice. In mRNA level, RAS+TSG-6 showed downregulated expression of all the inflammatory markers and TLR4/My88. TSG-6 was mainly expressed in renal tubular and interstitial cells and similarly in normal and RAS kidneys, but its expression was augmented in both sham and RAS mice treated with i.p. TSG-6 injections. Both mRNA and protein expression of CHOP and GRP78 were increased in RAS and were alleviated in RAS+TSG-6. Data are represented as mean ± SD. *$p < 0.05$, **$p < 0.01$, ***$p < 0.001$, ****$p < 0.0001$, comparisons were performed using one-way ANOVA followed by Fisher's LSD test, n = 5–6 mice/group.

TLR4 and MyD88 activates NF-κB, increasing the production of inflammatory and fibrotic factors.[27] The TLR4/MyD88/TRAF6/NF-κB pathway is also activated in the adenine-induced chronic kidney disease (CKD) in rats.[28] Our *in vitro* study confirmed that TSG-6 inhibits NF-κB at least in part through TLR4, whereas suppression of TNF-α expression was unlikely achieved through this pathway. Hence, while the TLR4/NF-κB inflammatory pathway is prominently involved in mediating the effects of TSG-6, it clearly confers anti-inflammatory effects via additional mechanisms.

We have previously shown that blood oxygenation level-dependent (BOLD)-determined hypoxia correlates with renal vein MCP-1 and neutrophil gelatinase-associated lipocalin levels.[29] In the current study, TSG-6 treatment reduced cortical and medullary hypoxia in the stenotic kidney, which may also be attributed to the improvement of the inflammatory microenvironment. Contrarily, it did not affect renal perfusion, suggesting that the decreased hypoxia may be linked to improved metabolic efficiencies in tubular transport activities rather than expanded microcirculation.

Apoptosis develops in response to cellular damage including inflammation. TNF-α plays a role in mediating apoptosis in renal tubular cells induced by unilateral ureteral obstruction and proapoptotic signaling,[30] and RAS increases the numbers of TUNEL+ and caspase-3+ cells.[22] Furthermore, apoptosis directly or indirectly promotes the inflammation induced by renal ischemia-reperfusion and subsequent tissue damage.[31] Our results indicated that TSG-6 effectively mitigates stenotic kidney apoptosis in mice and downregulates the key transcription factors ATF4, ATF5, and CHOP, key components of the ERS and mtUPR that are both associated with apoptosis.[32,33]

Many stresses encountered upon kidney damage are prone to trigger ERS,[34] which initiates and advances kidney diseases by promoting inflammation and apoptosis. Diabetic rats develop enhanced kidney cell apoptosis secondary to ERS, as evidenced by increased expression of CHOP, c-Jun N-terminal kinase

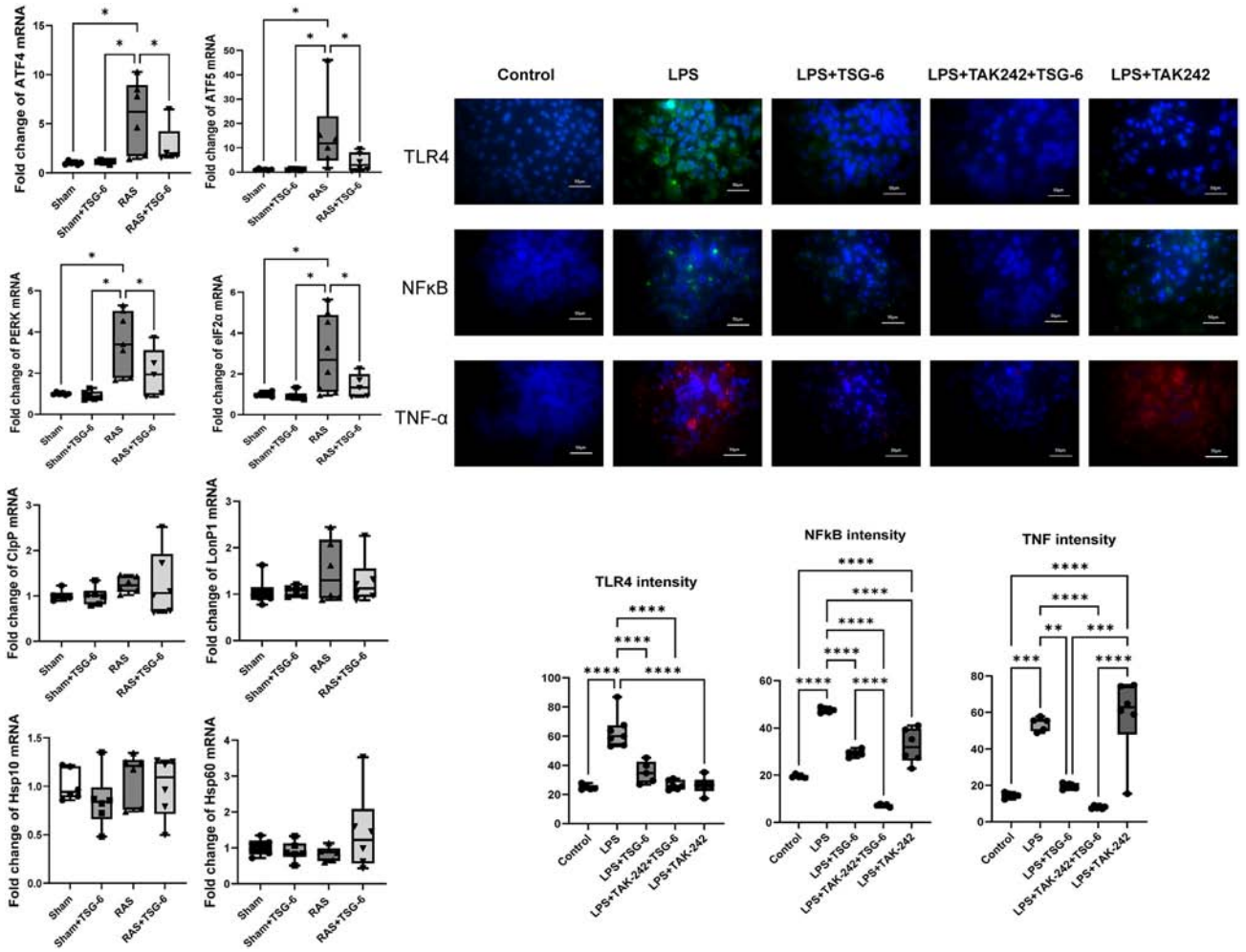

Figure 5. Renal mRNA expression of ERS and mtUPR genes *in vivo* and the effect of TSG-6 on the TLR4/NF-κB inflammatory pathway *in vitro*

Left, TSG-6 downregulated the elevated ATF4, ATF5, PERK, and eIF2α mRNA expression observed in the stenotic murine kidney. The mRNA expression of ClpP, LonP1, Hsp60, and Hsp10 remained unaltered. Right, in HK-2 cells, LPS upregulated both TLR4 and NF-κB expression. TSG-6 treatment alone abolished LPS-stimulated TLR4 and decreased NF-κB expression to levels no longer elevated vs. control, while its combination with TLR4 inhibition further abolished NF-κB expression. TGS-6 treatment significantly decreased TNF-α expression, whereas TAK-242 alone did not. Data are represented as mean ± SD. $^{*}p < 0.05$, $^{**}p < 0.01$, $^{***}p < 0.001$, $^{****}p < 0.0001$, comparisons were performed using one-way ANOVA followed by Fisher's LSD test, $n = 5$–6 mice/group or $n = 6$ samples.

(JNK), and caspase-12.[13] TNF-α, primarily produced by activated macrophages in stenotic mouse kidneys, induces apoptosis through ERS by upregulating CHOP and GRP94 expression.[35,36] Importantly, MSCs downregulate CHOP and GRP94 expression in the stenotic kidneys ER and bestow protective effects on renal tubular cell apoptosis induced by thapsigargin-induced ERS.[25] Pertinently, TSG-6 released from MSCs exhibits anti-inflammation properties in RAS.[5] In spinal cord ischemia-reperfusion damage, TSG-6 released from adipose MSC-derived extracellular vesicles exerts protective effects by inhibiting ERS.[20] Our current study extends previous studies and demonstrates that TSG-6 attenuates RAS-induced kidney damage in association with inhibiting ERS and apoptosis. Notably, elevated urinary protein excretion is associated with tubular damage and ERS.[37,38] We found that TSG-6 delivery reduced the elevated proteinuria levels in RAS, possibly due to the improvement of ERS. Thus, the ability of TSG-6 to alleviate ERS may reflect a broader impact on cellular homeostasis, contributing to its overall remedial effects in the context of ischemic kidney disease.

The ERS shares common mediators with the cellular process mtUPR. Mitochondria possess a unique set of chaperones responsible for the import, refolding, and prevention of protein aggregation. Disruption of this mechanism triggers the mtUPR, characterized by the upregulation of mitochondrial chaperones such as Hsp60 and proteases like LonP1.[39,40] While a moderate mtUPR can mitigate the initial damage and confer protective effects,[41,42] extensive or prolonged activation is detrimental and counterproductive.[43] Recent studies suggest that the mtUPR may play a role in cell death, potentially linked to the increased expression of CHOP.[44] ERS can cause eIF2α phosphorylation

through integrated stress response, which further upregulates the translation of mediators like CHOP, ATF4, and ATF5 that are transferred to the nucleus to initiate transcription of mtUPR-related genes.[45,46] Hence, mitochondrial stress may be a consequence of ERS. Interestingly, the mtUPR markers remained unaltered in RAS, implying that mtUPR is not activated or at least is preceded by ERS in our model of early RAS. Further investigations are warranted to unravel the specific interplay between ERS and mitochondrial function in the ischemic renal tissue.

In conclusion, our study underscores the reno-protective effects of TSG-6 in murine RAS, positioning it as a potential strategy to arrest stenotic kidney damage in renovascular disease. Its ability to enhance renal function, mitigate fibrosis and apoptosis, and modulate inflammatory and ERS pathways demonstrates its multifaceted therapeutic potential. Further studies are needed to verify its potential favorable influence on human RAS.

Limitations of the study

Despite our promising findings, we need to acknowledge the limitations of our study. The mouse model may not fully recapitulate the complexity of human renal diseases, and the extrapolation to clinical settings requires careful consideration. Given the small size and limited tissue availability of the atrophied stenotic kidneys, we focused on gene expression and on protein expression using immunostaining that requires smaller samples than western blotting. Although TSG-6 improved renal oxygenation, inflammation, and apoptosis in stenotic kidneys, it only slightly attenuated renovascular hypertension, which might necessitate multiple injections or higher doses of TSG-6. Additionally, future research also needs to explore the potential interaction between ERS and mtUPR.

RESOURCE AVAILABILITY

Lead contact

Further information and requests for resources and reagents should be directed to and will be fulfilled by the lead contact, Lilach O. Lerman (Lerman.Lilach@mayo.edu).

Materials availability

This study did not generate new unique reagents.

Data and code availability

- Data: Any information required to reanalyze the data reported in this work is available from the lead contact upon request.
- Code: This paper does not report original code.
- Other items: Any additional information required to reanalyze the data reported in this paper is available from the lead contact upon request

ACKNOWLEDGMENTS

This study was partly supported by NIH grant numbers DK120292, DK122734, HL158691, AG062104, and R25-DK101405.

AUTHOR CONTRIBUTIONS

All authors researched data for the article, contributed substantially to discussion of the content, wrote the article, and reviewed and/or edited the manuscript before submission.

DECLARATION OF INTERESTS

The authors declare no competing interests.

STAR★METHODS

Detailed methods are provided in the online version of this paper and include the following:

- KEY RESOURCES TABLE
- EXPERIMENTAL MODEL AND STUDY PARTICIPANT DETAILS
- METHOD DETAILS
  - Systemic measurements
  - MRI-derived renal function
  - Histological staining
  - Immunofluorescence staining
  - Real-time PCR (PCR)
  - In-vitro study
- QUANTIFICATION AND STATISTICAL ANALYSIS

SUPPLEMENTAL INFORMATION

Supplemental information can be found online at https://doi.org/10.1016/j.isci.2024.111454.

Received: July 5, 2024
Revised: September 20, 2024
Accepted: November 19, 2024
Published: November 22, 2024

REFERENCES

1. de Mast, Q., and Beutler, J.J. (2009). The prevalence of atherosclerotic renal artery stenosis in risk groups: a systematic literature review. J. Hypertens. *27*, 1333–1340. https://doi.org/10.1097/HJH.0b013e328329bbf4.
2. Riaz, I.B., Husnain, M., Riaz, H., Asawaeer, M., Bilal, J., Pandit, A., Shetty, R., and Lee, K.S. (2014). Meta-analysis of revascularization versus medical therapy for atherosclerotic renal artery stenosis. Am. J. Cardiol. *114*, 1116–1123. https://doi.org/10.1016/j.amjcard.2014.06.033.
3. Eirin, A., Zhu, X.Y., Urbieta-Caceres, V.H., Grande, J.P., Lerman, A., Textor, S.C., and Lerman, L.O. (2011). Persistent kidney dysfunction in swine renal artery stenosis correlates with outer cortical microvascular remodeling. Am. J. Physiol. Ren. Physiol. *300*, F1394–F1401. https://doi.org/10.1152/ajprenal.00697.2010.
4. Eirin, A., Zhu, X.Y., Puranik, A.S., Tang, H., McGurren, K.A., van Wijnen, A.J., Lerman, A., and Lerman, L.O. (2017). Mesenchymal stem cell-derived extracellular vesicles attenuate kidney inflammation. Kidney Int. *92*, 114–124. https://doi.org/10.1016/j.kint.2016.12.023.
5. Zhao, Y., Zhu, X.Y., Song, T., Zhang, L., Eirin, A., Conley, S., Tang, H., Saadiq, I., Jordan, K., Lerman, A., and Lerman, L.O. (2021). Mesenchymal stem cells protect renal tubular cells via TSG-6 regulating macrophage function and phenotype switching. Am. J. Physiol. Ren. Physiol. *320*, F454–F463. https://doi.org/10.1152/ajprenal.00426.2020.
6. Foskett, A.M., Bazhanov, N., Ti, X., Tiblow, A., Bartosh, T.J., and Prockop, D.J. (2014). Phase-directed therapy: TSG-6 targeted to early inflammation improves bleomycin-injured lungs. Am. J. Physiol. Lung Cell Mol. Physiol. *306*, L120–L131. https://doi.org/10.1152/ajplung.00240.2013.
7. Milner, C.M., and Day, A.J. (2003). TSG-6: a multifunctional protein associated with inflammation. J. Cell Sci. *116*, 1863–1873. https://doi.org/10.1242/jcs.00407.
8. Janssen, U., Thomas, G., Glant, T., and Phillips, A. (2001). Expression of inter-alpha-trypsin inhibitor and tumor necrosis factor-stimulated gene 6 in renal proximal tubular epithelial cells. Kidney Int. *60*, 126–136. https://doi.org/10.1046/j.1523-1755.2001.00779.x.

9. Kato, T., Okumi, M., Tanemura, M., Yazawa, K., Kakuta, Y., Yamanaka, K., Tsutahara, K., Doki, Y., Mori, M., Takahara, S., and Nonomura, N. (2014). Adipose tissue-derived stem cells suppress acute cellular rejection by TSG-6 and CD44 interaction in rat kidney transplantation. Transplantation *98*, 277–284. https://doi.org/10.1097/TP.0000000000000230.

10. Wu, H.J., Yiu, W.H., Li, R.X., Wong, D.W.L., Leung, J.C.K., Chan, L.Y.Y., Zhang, Y., Lian, Q., Lin, M., Tse, H.F., et al. (2014). Mesenchymal stem cells modulate albumin-induced renal tubular inflammation and fibrosis. PLoS One *9*, e90883. https://doi.org/10.1371/journal.pone.0090883.

11. Zhang, K., and Kaufman, R.J. (2006). The unfolded protein response: a stress signaling pathway critical for health and disease. Neurology *66*, S102–S109. https://doi.org/10.1212/01.wnl.0000192306.98198.

12. Chaudhari, N., Talwar, P., Parimisetty, A., Lefebvre d'Hellencourt, C., and Ravanan, P. (2014). A molecular web: endoplasmic reticulum stress, inflammation, and oxidative stress. Front. Cell. Neurosci. *8*, 213. https://doi.org/10.3389/fncel.2014.00213.

13. Liu, G., Sun, Y., Li, Z., Song, T., Wang, H., Zhang, Y., and Ge, Z. (2008). Apoptosis induced by endoplasmic reticulum stress involved in diabetic kidney disease. Biochem. Biophys. Res. Commun. *370*, 651–656. https://doi.org/10.1016/j.bbrc.2008.04.031.

14. Gao, X., Fu, L., Xiao, M., Xu, C., Sun, L., Zhang, T., Zheng, F., and Mei, C. (2012). The nephroprotective effect of tauroursodeoxycholic acid on ischaemia/reperfusion-induced acute kidney injury by inhibiting endoplasmic reticulum stress. Basic Clin. Pharmacol. Toxicol. *111*, 14–23. https://doi.org/10.1111/j.1742-7843.2011.00854.x.

15. Zhao, M., Wang, Y., Li, L., Liu, S., Wang, C., Yuan, Y., Yang, G., Chen, Y., Cheng, J., Lu, Y., and Liu, J. (2021). Mitochondrial ROS promote mitochondrial dysfunction and inflammation in ischemic acute kidney injury by disrupting TFAM-mediated mtDNA maintenance. Theranostics *11*, 1845–1863. https://doi.org/10.7150/thno.50905.

16. Farahani, R.A., Zhu, X.Y., Tang, H., Jordan, K.L., Lerman, L.O., and Eirin, A. (2020). Renal ischemia alters expression of mitochondria-related genes and impairs mitochondrial structure and function in swine scattered tubular-like cells. Am. J. Physiol. Ren. Physiol. *319*, F19–F28. https://doi.org/10.1152/ajprenal.00120.2020.

17. Lim, Y., Berry, B., Viteri, S., McCall, M., Park, E.C., Rongo, C., Brookes, P.S., and Nehrke, K. (2021). FNDC-1-mediated mitophagy and ATFS-1 coordinate to protect against hypoxia-reoxygenation. Autophagy *17*, 3389–3401. https://doi.org/10.1080/15548627.2021.1872885.

18. Voos, W., Jaworek, W., Wilkening, A., and Bruderek, M. (2016). Protein quality control at the mitochondrion. Essays Biochem. *60*, 213–225. https://doi.org/10.1042/ebc20160009.

19. Martínez-Klimova, E., Aparicio-Trejo, O.E., Gómez-Sierra, T., Jiménez-Uribe, A.P., Bellido, B., and Pedraza-Chaverri, J. (2020). Mitochondrial dysfunction and endoplasmic reticulum stress in the promotion of fibrosis in obstructive nephropathy induced by unilateral ureteral obstruction. Biofactors *46*, 716–733. https://doi.org/10.1002/biof.1673.

20. Lu, X., Lv, C., Zhao, Y., Wang, Y., Li, Y., Ji, C., Wang, Z., Ye, W., Yu, S., Bai, J., and Cai, W. (2022). TSG-6 released from adipose stem cells-derived small extracellular vesicle protects against spinal cord ischemia reperfusion injury by inhibiting endoplasmic reticulum stress. Stem Cell Res. Ther. *13*, 291. https://doi.org/10.1186/s13287-022-02963-4.

21. Zhu, X.Y., Chade, A.R., Rodriguez-Porcel, M., Bentley, M.D., Ritman, E.L., Lerman, A., and Lerman, L.O. (2004). Cortical microvascular remodeling in the stenotic kidney: role of increased oxidative stress. Arterioscler. Thromb. Vasc. Biol. *24*, 1854–1859. https://doi.org/10.1161/01.ATV.0000142443.52606.81.

22. Song, T., Zhu, X.Y., Eirin, A., Jiang, Y., Krier, J.D., Tang, H., Jordan, K.L., Lerman, A., and Lerman, L.O. (2022). Exogenous pericyte delivery protects the mouse kidney from chronic ischemic injury. Am. J. Physiol. Ren. Physiol. *323*, F527–F538. https://doi.org/10.1152/ajprenal.00064.2022.

23. Jo, S.K., Sung, S.A., Cho, W.Y., Go, K.J., and Kim, H.K. (2006). Macrophages contribute to the initiation of ischaemic acute renal failure in rats. Nephrol. Dial. Transplant. *21*, 1231–1239. https://doi.org/10.1093/ndt/gfk047.

24. Burne-Taney, M.J., Kofler, J., Yokota, N., Weisfeldt, M., Traystman, R.J., and Rabb, H. (2003). Acute renal failure after whole body ischemia is characterized by inflammation and T cell-mediated injury. Am. J. Physiol. Ren. Physiol. *285*, F87–F94. https://doi.org/10.1152/ajprenal.00026.2003.

25. Zhu, X.Y., Urbieta-Caceres, V., Krier, J.D., Textor, S.C., Lerman, A., and Lerman, L.O. (2013). Mesenchymal Stem Cells and Endothelial Progenitor Cells Decrease Renal Injury in Experimental Swine Renal Artery Stenosis Through Different Mechanisms. Stem Cell. *31*, 117–125. https://doi.org/10.1002/stem.1263.

26. Iwasaki, A., and Medzhitov, R. (2004). Toll-like receptor control of the adaptive immune responses. Nat. Immunol. *5*, 987–995. https://doi.org/10.1038/ni1112.

27. Lin, K., Luo, W., Yang, N., Su, L., Zhou, H., Hu, X., Wang, Y., Khan, Z.A., Huang, W., Wu, G., and Liang, G. (2022). Inhibition of MyD88 attenuates angiotensin II-induced hypertensive kidney disease via regulating renal inflammation. Int. Immunopharm. *112*, 109218. https://doi.org/10.1016/j.intimp.2022.109218.

28. Samaha, M.M., Nour, O.A., Sewilam, H.M., and El-Kashef, D.H. (2023). Diacerein mitigates adenine-induced chronic kidney disease in rats: Focus on TLR4/MYD88/TRAF6/NF-kappaB pathway. Life Sci. *331*, 122080. https://doi.org/10.1016/j.lfs.2023.122080.

29. Abumoawad, A., Saad, A., Ferguson, C.M., Eirin, A., Woollard, J.R., Herrmann, S.M., Hickson, L.J., Bendel, E.C., Misra, S., Glockner, J., et al. (2019). Tissue hypoxia, inflammation, and loss of glomerular filtration rate in human atherosclerotic renovascular disease. Kidney Int. *95*, 948–957. https://doi.org/10.1016/j.kint.2018.11.039.

30. Misseri, R., Meldrum, D.R., Dinarello, C.A., Dagher, P., Hile, K.L., Rink, R.C., and Meldrum, K.K. (2005). TNF-alpha mediates obstruction-induced renal tubular cell apoptosis and proapoptotic signaling. Am. J. Physiol. Ren. Physiol. *288*, F406–F411. https://doi.org/10.1152/ajprenal.00099.2004.

31. Daemen, M.A., van 't Veer, C., Denecker, G., Heemskerk, V.H., Wolfs, T.G., Clauss, M., Vandenabeele, P., and Buurman, W.A. (1999). Inhibition of apoptosis induced by ischemia-reperfusion prevents inflammation. J. Clin. Invest. *104*, 541–549. https://doi.org/10.1172/jci6974.

32. Lian, X., Wang, X., Xie, Y., Sheng, H., He, J., Peng, T., Xie, N., Wang, C., and Lian, Y. (2024). ATF5-regulated Mitochondrial Unfolded Protein Response Attenuates Neuronal Damage in Epileptic Rat by Reducing Endoplasmic Reticulum Stress Through Mitochondrial ROS. Neurochem. Res. *49*, 388–401. https://doi.org/10.1007/s11064-023-04042-3.

33. Anderson, N.S., and Haynes, C.M. (2020). Folding the Mitochondrial UPR into the Integrated Stress Response. Trends Cell Biol. *30*, 428–439. https://doi.org/10.1016/j.tcb.2020.03.001.

34. Gallazzini, M., and Pallet, N. (2018). Endoplasmic reticulum stress and kidney dysfunction. Biol. Cell *110*, 205–216. https://doi.org/10.1111/boc.201800019.

35. Chiribau, C.B., Gaccioli, F., Huang, C.C., Yuan, C.L., and Hatzoglou, M. (2010). Molecular symbiosis of CHOP and C/EBP beta isoform LIP contributes to endoplasmic reticulum stress-induced apoptosis. Mol. Cell Biol. *30*, 3722–3731. https://doi.org/10.1128/mcb.01507-09.

36. Yamaguchi, H., and Wang, H.G. (2004). CHOP is involved in endoplasmic reticulum stress-induced apoptosis by enhancing DR5 expression in human carcinoma cells. J. Biol. Chem. *279*, 45495–45502. https://doi.org/10.1074/jbc.M406933200.

37. Cybulsky, A.V. (2010). Endoplasmic reticulum stress in proteinuric kidney disease. Kidney Int. *77*, 187–193. https://doi.org/10.1038/ki.2009.389.

38. Lee, E.K., Jeong, J.U., Chang, J.W., Yang, W.S., Kim, S.B., Park, S.K., Park, J.S., and Lee, S.K. (2012). Activation of AMP-Activated Protein Kinase Inhibits Albumin-Induced Endoplasmic Reticulum Stress and Apoptosis through Inhibition of Reactive Oxygen Species. Nephron Exp. Nephrol. *121*, E38–E48. https://doi.org/10.1159/000342802.

39. Maity, S., Basak, T., Bhat, A., Bhasin, N., Ghosh, A., Chakraborty, K., and Sengupta, S. (2014). Cross-compartment proteostasis regulation during redox imbalance induced ER stress. Proteomics *14*, 1724–1736. https://doi.org/10.1002/pmic.201300449.

40. Yoneda, T., Benedetti, C., Urano, F., Clark, S.G., Harding, H.P., and Ron, D. (2004). Compartment-specific perturbation of protein handling activates genes encoding mitochondrial chaperones. J. Cell Sci. *117*, 4055–4066. https://doi.org/10.1242/jcs.01275.

41. Durieux, J., Wolff, S., and Dillin, A. (2011). The cell-non-autonomous nature of electron transport chain-mediated longevity. Cell *144*, 79–91. https://doi.org/10.1016/j.cell.2010.12.016.

42. Houtkooper, R.H., Mouchiroud, L., Ryu, D., Moullan, N., Katsyuba, E., Knott, G., Williams, R.W., and Auwerx, J. (2013). Mitonuclear protein imbalance as a conserved longevity mechanism. Nature *497*, 451–457. https://doi.org/10.1038/nature12188.

43. Moullan, N., Mouchiroud, L., Wang, X., Ryu, D., Williams, E.G., Mottis, A., Jovaisaite, V., Frochaux, M.V., Quiros, P.M., Deplancke, B., et al. (2015). Tetracyclines disturb mitochondrial function across eukaryotic models: a call for caution in biomedical research. Cell Rep. *10*, 1681–1691. https://doi.org/10.1016/j.celrep.2015.02.034.

44. Siegelin, M.D., Dohi, T., Raskett, C.M., Orlowski, G.M., Powers, C.M., Gilbert, C.A., Ross, A.H., Plescia, J., and Altieri, D.C. (2011). Exploiting the mitochondrial unfolded protein response for cancer therapy in mice and human cells. J. Clin. Invest. *121*, 1349–1360. https://doi.org/10.1172/jci44855.

45. Smyrnias, I. (2021). The mitochondrial unfolded protein response and its diverse roles in cellular stress. Int. J. Biochem. Cell Biol. *133*, 105934. https://doi.org/10.1016/j.biocel.2021.105934.

46. Zhang, P., McGrath, B., Li, S., Frank, A., Zambito, F., Reinert, J., Gannon, M., Ma, K., McNaughton, K., and Cavener, D.R. (2002). The PERK eukaryotic initiation factor 2 alpha kinase is required for the development of the skeletal system, postnatal growth, and the function and viability of the pancreas. Mol. Cell Biol. *22*, 3864–3874. https://doi.org/10.1128/mcb.22.11.3864-3874.2002.

47. Siddiqi, S., Klomjit, N., Jiang, K., Conley, S.M., Zhu, X., Saadiq, I.M., Ferguson, C.M., Tang, H., Lerman, A., and Lerman, L.O. (2023). Efficacy of human embryonic stem Cells compared to adipose tissue-derived Human mesenchymal stem/stromal cells for repair of murine post-stenotic kidneys. Stem Cell Rev. Rep. *19*, 491–502. https://doi.org/10.1007/s12015-022-10443-8.

48. Eirin, A., Ebrahimi, B., Zhang, X., Zhu, X.Y., Woollard, J.R., He, Q., Textor, S.C., Lerman, A., and Lerman, L.O. (2014). Mitochondrial protection restores renal function in swine atherosclerotic renovascular disease. Cardiovasc. Res. *103*, 461–472. https://doi.org/10.1093/cvr/cvu157.

49. Mittal, M., Tiruppathi, C., Nepal, S., Zhao, Y.Y., Grzych, D., Soni, D., Prockop, D.J., and Malik, A.B. (2016). TNFalpha-stimulated gene-6 (TSG6) activates macrophage phenotype transition to prevent inflammatory lung injury. Proc. Natl. Acad. Sci. USA *113*, E8151–E8158. https://doi.org/10.1073/pnas.1614935113.

50. Yang, H., Feng, R., Fu, Q., Xu, S., Hao, X., Qiu, Y., Feng, T., Zeng, Z., Chen, M., and Zhang, S. (2019). Human induced pluripotent stem cell-derived mesenchymal stem cells promote healing via TNF-alpha-stimulated gene-6 in inflammatory bowel disease models. Cell Death Dis. *10*, 718. https://doi.org/10.1038/s41419-019-1957-7.

51. Percie du Sert, N., Hurst, V., Ahluwalia, A., Alam, S., Avey, M.T., Baker, M., Browne, W.J., Clark, A., Cuthill, I.C., Dirnagl, U., et al. (2020). The ARRIVE guidelines 2.0: updated guidelines for reporting animal research. BMJ Open Sci. *4*, e100115. https://doi.org/10.1136/bmjos-2020-100115.

52. Cheng, J., Zhou, W., Warner, G.M., Knudsen, B.E., Garovic, V.D., Gray, C.E., Lerman, L.O., Platt, J.L., Romero, J.C., Textor, S.C., et al. (2009). Temporal analysis of signaling pathways activated in a murine model of two-kidney, one-clip hypertension. Am. J. Physiol. Ren. Physiol. *297*, F1055–F1068. https://doi.org/10.1152/ajprenal.90439.2008.

53. Kim, S.R., Puranik, A.S., Jiang, K., Chen, X., Zhu, X.Y., Taylor, I., Khodadadi-Jamayran, A., Lerman, A., Hickson, L.J., Childs, B.G., et al. (2021). Progressive Cellular Senescence Mediates Renal Dysfunction in Ischemic Nephropathy. J. Am. Soc. Nephrol. *32*, 1987–2004. https://doi.org/10.1681/ASN.2020091373.

54. Ebrahimi, B., Crane, J.A., Knudsen, B.E., Macura, S.I., Grande, J.P., and Lerman, L.O. (2013). Evolution of cardiac and renal impairment detected by high-field cardiovascular magnetic resonance in mice with renal artery stenosis. J. Cardiovasc. Magn. Reson. *15*, 98. https://doi.org/10.1186/1532-429x-15-98.

55. Jiang, K., Ferguson, C.M., Ebrahimi, B., Tang, H., Kline, T.L., Burningham, T.A., Mishra, P.K., Grande, J.P., Macura, S.I., and Lerman, L.O. (2017). Noninvasive assessment of renal fibrosis with magnetization transfer MR imaging: validation and evaluation in murine renal artery stenosis. Radiology *283*, 77–86. https://doi.org/10.1148/radiol.2016160566.

56. Hu, M., Wei, J., Yang, L., Xu, J., He, Z., Li, H., Ning, C., and Lu, S. (2021). Linc-KIAA1737-2 promoted LPS-induced HK-2 cell apoptosis by regulating miR-27a-3p/TLR4/NF-kappaB axis. J. Bioenerg. Biomembr. *53*, 393–403. https://doi.org/10.1007/s10863-021-09897-1.

57. Nakazawa, D., Takeda, Y., Kanda, M., Tomaru, U., Ogawa, H., Kudo, T., Shiratori-Aso, S., Watanabe-Kusunoki, K., Ueda, Y., Miyoshi, A., et al. (2023). Inhibition of Toll-like receptor 4 and Interleukin-1 receptor prevent SARS-CoV-2 mediated kidney injury. Cell Death Dis. *9*, 293. https://doi.org/10.1038/s41420-023-01584-x.

STAR★METHODS

KEY RESOURCES TABLE

REAGENT or RESOURCE	SOURCE	IDENTIFIER
Antibodies		
F4/80 antibody	Abcam	Cat#ab6640; RRID:AB_1140040
Mannose receptor-1 (MRC-1) antibody	Sigma-Aldrich	Cat#HPA004114; RRID:AB_1846270
iNOS antibody	Santa Cruz Biotechnology	Cat#SC-7271; RRID:AB_627810
TSG-6 antibody	Santa Cruz Biotechnology	Cat#sc398307
TLR4 antibody	Novus Biologicals	Cat#NB100-56566; RRID:AB_2205129
TNF-α antibody	Affinity Biosciences	Cat#CRG0511071
NF-κB antibody	Abcam	Cat#ab106129; RRID:AB_10902018
CHOP antibody	LifeSpan BioSciences	Cat#LS-C352113
GRP78 antibody	Abcam	Cat#ab21685; RRID:AB_2119834
Chemicals, peptides, and recombinant proteins		
Recombinant human TSG-6	R&D Systems	Cat#2104-TS
Critical commercial assays		
TAK-242	EMD Millipore	Cat#614316
DetectX Serum Creatinine kit	Arbor Assays	KB02-H1
Pierce BCA Protein Assay kit	Thermo Fisher	Cat#23225
TUNEL Apoptosis Detection Kit	Promega	Cat#G3250
Total RNA Extraction Kit	Thermo Fisher	AM1556
SuperScript VILO cDNA Synthesis Kit	Thermo Fisher	Cat#11754-050
NF-κB Taqman Assay	Thermo Fisher	mm00476361
MyD88 Taqman Assay	Thermo Fisher	mm00440338
TLR4 Taqman Assay	Thermo Fisher	mm00445273
TNF-α Taqman Assay	Thermo Fisher	mm00443258
ATF4 Taqman Assay	Thermo Fisher	mm00515325
ATF5 Taqman Assay	Thermo Fisher	mm04179654
GRP78 Taqman Assay	Thermo Fisher	mm00517691
PERK Taqman Assay	Thermo Fisher	mm00438700
eIF2α Taqman Assay	Thermo Fisher	mm01289723
CHOP Taqman Assay	Thermo Fisher	mm01135937
ClpP Taqman Assay	Thermo Fisher	mm00489940
LonP1 Taqman Assay	Thermo Fisher	mm01236887
HSP60 Taqman Assay	Thermo Fisher	mm00849835
HSP10 Taqman Assay	Thermo Fisher	mm07295795
GAPDH Taqman Assay	Thermo Fisher	mm99999915
Experimental models: Cell lines		
Human: HK-2	ATCC	CRL-2190
Experimental models: Organisms/strains		
Mouse: male S129	Jackson Laboratory	002448
Software and algorithms		
ZEN Microscopy software https://www.zeiss.com/microscopy/en/products/software/zeiss-zen.html	ZEISS	RRID:SCR_013672
GraphPad Prism http://www.graphpad.com/	GraphPad	RRID:SCR_002798

(*Continued on next page*)

Continued

REAGENT or RESOURCE	SOURCE	IDENTIFIER
ImageJ software https://imagej.net/	NIH	RRID:SCR_003070
MATLAB software http://www.mathworks.com/products/matlab/	MathWorks	RRID:SCR_001622
Nikon NIS-Elements AR Analysis software	Nikon	Version 5.42.02
SPSS Statistics http://www-01.ibm.com/software/uk/analytics/spss/	IBM	RRID:SCR_002865 v.29 software
Other		
DMEM/F12 medium	Thermo Fisher	Cat#10565-018
Fetal Bovine Serum (FBS)	Thermo Fisher	Cat#26140-079
Lipopolysaccharide (LPS)	Sigma-Aldrich	Cat#L4524
DAPI	Thermo Fisher	Cat#P36935
Nikon Fluorescence Microscope	Nikon	Eclipse Ci
Nikon microscope	Nikon	Eclipse Ci
PBS	Thermo Fisher	Cat#14190-144
CODA High Throughput System (blood pressure measurement)	Kent Scientific	CODA 21804
MRI System	Bruker	Ultrashied^{TM} 700WB Plus
Zeiss Microscope	Carl Zeiss	Observer Z1

EXPERIMENTAL MODEL AND STUDY PARTICIPANT DETAILS

Twenty-four male or female S129 mice, 11 weeks old (Jackson Laboratory, Bar Harbor, ME), were housed in groups of 3–4 per cage at a temperature of 21°C–23°C, following a 12-h light/dark cycle, with unrestricted access to city water and standard chow (Figure 1A). Acute experiments were carried out in a designated animal surgery suite in the late morning, around 11 a.m. RAS was induced in 12 mice using the two-kidney one-cuff model.[47] After isoflurane anesthesia (1.5–2.0%), the right kidney was exposed and the renal artery isolated. A 0.2 mm diameter, 0.5mm-long cuff (Polyetrafluoroethylene, Braintree Scientific, Braintree, MA) cut longitudinally was placed around the renal artery, and secured with nylon suture. The kidney was returned and the incisions sutured. Successful RAS surgery was confirmed by subsequent right-to-left volume or weight ratio of less than 0.9, and no mice were excluded in this study. A sham surgery was performed in 12 mice. Two weeks after surgery, RAS and sham mice were randomly assigned to TSG-6 or vehicle treatment (n = 6 each group, based on our previous studies in which the inclusion of 6 animals allowed detecting statistically significant changes in RAS kidney).[48] Recombinant human TSG-6 (rhTSG-6; 5μg/200μL PBS; R&D, Minneapolis, MN)[49,50] was administered intra-peritoneally (IP) to 6 RAS and 6 sham mice every other day 7 times over two weeks. The control mice (6 RAS and 6 sham) received 7 IP injections each of 200uL PBS. The ARRIVE reporting guidelines were used in this paper[51] (Data S1). All procedures (including procedures reducing pain, suffering and distress) were approved by the Mayo Clinic Institutional Animal Care and Use Committee (A00006226-21).

METHOD DETAILS

Systemic measurements

Blood pressure measurements were taken using the tail cuff method at baseline, 2 weeks, and 4 weeks post-surgery around 9 a.m. with the CODA High Throughput system (Kent Scientific, Torrington, CT).[52] Blood and urine samples were collected prior to euthanasia. Plasma creatinine levels were measured with the DetectX Serum Creatinine kit (Arbor Assays, Ann Arbor, MI), and urine protein levels were determined using the Pierce BCA protein assay kit (ThermoFisher, Cat#23225).[53]

MRI-derived renal function

After completing the regimen, all mice underwent 16.4-T magnetic resonance imaging (MRI) scans to evaluate renal oxygenation, perfusion, and blood flow. The mice were anesthetized with 1.0–2.0% isoflurane and their ECG, respiration, and body temperature were continuously monitored (SA Instruments, Stony Brook, NY). A vertical animal scanner with a 38-mm inner diameter birdcage coil (Bruker, Billerica, MA) was utilized. Renal volume was assessed using coronal images captured by a respiration-gated three-dimensional fast imaging sequence with steady precession. Arterial spin labeling with the flow-sensitive alternating inversion-recovery sequence was employed to measure renal perfusion and blood flow. Renal oxygenation was measured by blood-oxygen-level-dependent MRI using

a respiration-gated three-dimensional multi-echo gradient echo sequence. ANALYZE software (version 12.0, Biomedical Imaging Resource, Mayo Clinic, MN) was used to quantify renal volumes, and all other MRI images were reconstructed and analyzed offline with software packages in MATLAB (The MathWorks, Natick, MA).[54,55]

Histological staining

Masson's trichrome staining was performed to evaluate renal fibrosis in paraffin-embedded kidney sections. Twenty randomly selected nonoverlapping fields from each kidney were analyzed in a blinded manner using ImageJ (National Institutes of Health). Fibrosis was measured by determining the proportion of the tissue cross-sectional area that exhibited positive staining.

Apoptosis was evaluated using immunofluorescence staining with terminal dUTP nick-end labeling (TUNEL) (cat#G3250, Promega) on 5-μm kidney cross sections. Positive cells were manually counted in 15–20 fields under fluorescence microscopy (ZEN 2012 Blue Edition, Carl Zeiss).[48]

Immunofluorescence staining

Macrophages can be classified roughly into a pro-inflammatory (M1) or anti-inflammatory (M2) phenotype. Kidney tissue was double-stained with F4/80 (macrophages) (cat#ab6640) and mannose receptor-1 (MRC-1) (M2) (cat#HPA004114-100UL) or inducible nitric oxide synthase (iNOS) (M1) (cat#SC-7271). After nuclear staining with DAPI, double immune-stained cells were visualized with a Nikon fluorescence microscope (40X). Ten randomly selected nonoverlapping images taken from each kidney were used to count M1 and M2 macrophages, and subsequently, the M1/M2 ratio was calculated. Furthermore, renal IF staining were performed to detect protein expressions of TSG-6 (sc398307, 1:50), toll-like receptor-4 (TLR4) (NB100-56566, 1:500), tumor necrosis factor-α (TNF-α) (CRG0511071, 1:200), nuclear factor kappa-light-chain-enhancer of activated B-Cells (NF-κB) (aliases *Nfkb*) (ab106129, 1:3000), C/EBP homologous protein (CHOP) (LS-C352113, 1:100), and glucose-regulated protein-78 (GRP78) (ab21685, 1:400). Images (10 per slide) were taken with a Nikon microscope and quantified using ImageJ.

Real-time PCR (PCR)

Total RNA was extracted from kidney tissue (ThermoFisher, AM1556), and superScript VILO cDNA Synthesis kit (Waltham, MA; ThermoFisher, cat#11754-050) was used to generate cDNA from 800/ng of total RNA. Quantitative PCR was conducted with Taqman assays (ThermoFisher) and primers for inflammatory markers such as *Nfkb* (mm00476361), myeloid differentiation primary response protein-88 (*Myd88*) (mm00440338), *Tlr4* (mm00445273), *Tnf* (aliases TNF-α) (mm00515325), and activating transcription factor-4 (*Atf4*) (mm00515325), ERS genes primers included activating transcription factor-5 (*Atf5*) (mm04179654), heat shock protein family-A member-5 (*Hspa5*) (aliases GRP78) (mm00517691), eukaryotic translation initiation factor-2 alpha kinase-3 (*Eif2ak3*) (aliases protein kinase R-like endoplasmic reticulum kinase, PERK) (mm00438700), eukaryotic translation initiation factor-2, subunit-1-alpha (*Eif2s1*) (aliases eukaryotic translation initiation factor-2α, eIF2α) (mm01289723), DNA-damage inducible transcript-3 (*Ddit3*) (aliases CHOP); mtUPR genes primers included caseinolytic mitochondrial matrix peptidase proteolytic subunit (*Clpp*) (mm00489940), Lon protease-1 (*Lonp1*) (mm01236887), heat shock protein-1 (chaperonin) (*Hspd1*) (aliases Hsp60) (mm00849835), heat shock protein-1 (chaperonin-10) (*Hspe1*) (aliases Hsp10) (mm07295795), and glyceraldehyde-3-phosphate dehydrogenase (*Gapdh*) (mm99999915). Relative mRNA levels were normalized to *Gapdh* mRNA by the $2^{-\Delta\Delta CT}$ method. Each sample was processed in duplicate.

In-vitro study

To establish a mechanistic role for TSG-6 through the TLR4/NF-κB inflammatory pathways, HK-2 (CRL-2190, ATCC) human adult male kidney cells were cultured in DMEM/F12 supplied with 10% FBS in chamber slides, 6 wells per group. Cells were treated with a TLR4 stimulator lipopolysaccharide (LPS, Sigma-Adrich, cat#L4524, 8μg/ml)[56] for 24h, or its inhibitor TAK-242 (EMD Millipore, cat#614316, 5μM)[57] for 72h, with or without adding TSG-6 (rhTSG-6, R&D Systems, 100 ng/ml) for 24h. Cells were then fixed and stained with antibodies against TLR4 (NB100-56566, 1:100), NF-κB (ab106129, 1:1000), and for comparison purposes also with TNF-α (CRG0511071, 1:100). Six images/well were taken with 40x lens in a Nikon microscope at the same exposure setting, and their average intensity was quantified using Nikon NIS-Elements AR Analysis version 5.42.02.

QUANTIFICATION AND STATISTICAL ANALYSIS

Statistical analysis was performed with GraphPad Prism-9 (GraphPad Software, San Diego, CA). Results are presented as mean ± SD. Statistical significance was evaluated using one-way analysis of variance (ANOVA), with the Least Significant Difference (LSD) method applied for comparison between two groups or a paired t-test between experimental periods. p values smaller than 0.05 were considered significant and are indicated in the Figure Legends with an asterisk; specifically, $^{*}p < 0.05$, $^{**}p < 0.01$, $^{***}p < 0.001$, $^{****}p < 0.0001$ denote increasing levels of significance. For each experiment, 'n' indicates the sample size (number of mice or experiments).